Some New Measurements of the Ground and $\nu_2 = 1$

States of HDO in the Region 200 – 750 GHz

By

Melissa A. Kelly

In partial fulfillment of the requirements

for the degree of Master of Science

California Institute of Technology

Pasadena, California

2002

Submitted 16 September 2002

Table of Contents

Acknowledgements

Thanks be to Geoffrey A. Blake, my advisor for the past year at Caltech, who gave me work to do, money with which to do it, answers to my many questions, and help through this experience. Thanks also to the Blake group for their sharing of knowledge and help, in the laboratory and in classes.

Particular thanks go to members of the Millimeter and Submillimeter Spectroscopy group at JPL. Pin Chen provided me with a terahertz spectrometer to develop, and also help with using the fitting programs. Brian Drouin allowed me to use his spectrometer and stood by my side throughout the measurements. Also thanks to Timothy Crawford, Herb Pickett, Chip Miller and John Pearson, who offered extensive help and advice.

Thanks to the SCA and the populace of the Kingdom of Caid, without whom I would have had nothing to do in my free time and would have snapped long ago. Thanks in particular to the rapier fighters, and all my sword fighting teachers, especially the Tattershall group. After a long day in the lab, there's nothing better than punking someone in the head with a little Fiore or Giganti to, ironically, bring my mind back to the real world. Thanks to my friends for their concern and diversions when I had about lost my mind.

Finally, unlimited thanks and love to my family: my Mom and Dad, my sister and my brothers for their undying support and help in getting me through this one step at a time. I could not have done it without you.

Abstract

To facilitate measurements of HDO in molecular clouds, late-type stars and planetary atmospheres, several new lines of HDO were measured between 200 and 750 GHz. The measurements were done in a one-meter gas flow cell, with specially constructed diode multiplier sources and a liquid helium cooled InSb hot-electron bolometer. The lines measured were of very low intensity, thanks to their higher J and K values. Both a-type and b-type transitions were observed, in the vibrational ground state (000) and the first excited bending state (010). These lines were added to existing HDO spectral lines and fit using a least-squares regression of an Euler series Hamiltonian that has proven useful in the analysis of molecules with large vibrational amplitudes. The results were comparable in precision to existing analyses. The data will be beneficial to two upcoming remote sensing missions designed to investigate the far IR and microwave regions: SOFIA, an airborne observatory that will carry a 2.5m telescope and detectors into the upper atmosphere, and the Herschel space observatory, a cryogenically cooled 3.5m telescope that will operate at the L2 Lagrangian point some 1.5 million km from the Earth.

Introduction

On the Nature of Spectroscopy

Since its origins in the 19th century, the use of spectroscopic techniques to investigate species in the laboratory, or in the far reaches of space, has had a profound effect on the physical sciences. Atoms and molecules, either ionized or neutral, exhibit features throughout most of the electromagnetic spectrum. From the high-energy x-rays produced by internal electron transitions to the low energy molecular rotations, each spectral line, whether emission or absorption, gives detailed information about the physical and chemical dynamics taking place. Studied primarily are dynamics shown by transitions in three regions: electronic structure (optical and UV range, $\lambda \sim 1$ μm to 100 nm), vibrational degrees of freedom (infra-red, or IR, $\lambda \sim 1 - 30$ μm), and rotational degrees of freedom (far IR and microwave, $\lambda \sim 100$ μm – 1000 mm).

Microwave spectroscopy got its start in 1934, with the observations by Cleeton and Williams of NH_3 contained in a rubber bag.[1] The next molecule to be observed was H_2O. During WWII the US Navy noticed highly attenuated radar signals near a wavelength of 1.3 cm—the radar frequency was one at which water vapor absorbs. This breakthrough enabled microwave spectroscopy to flourish after the war, using technologies developed for radar.[2] New microwave and far-IR source technologies—notably diode multipliers, optical-heterodyne conversion—have appeared and developed over the last few decades to broaden the accessible range, maximize power and reduce noise. However, microwave spectroscopy is a discipline that has not been entirely overhauled by new technology; some sources used half a century ago, such as klystron tubes, are still entirely valid.

The microwave and far-IR regions provide extensive molecular information. Line positions determine the rotational constants, and thereby the moments of inertia and molecular structure. In addition, some vibrational information is accessible, as the rotational constants have a dependence on the vibrational quantum numbers. The dipole moment[3] can be determined as well, by measuring the frequency shifts of lines in the applied electric field of a Stark-modulated spectrometer.[4] This method is highly superior to that of measuring dielectric constants; not only are the measurements immune to sample impurities, but, in mixtures, a species of low concentration can be accurately measured if its spectral lines are known. Beyond the rotations of molecules, at the high energy end of the range, one begins to investigate the barriers to internal rotation and torsional modes in stable molecules, as well as the intermolecular vibrations of van der Waals and hydrogen bonded clusters.

This research dealt with investigations of the deuterated water molecule, HDO, in the region between 200 and 750 GHz. Though at these frequencies the exact border between microwave and far-infrared is not institutionally defined, the experimental technique is effectively microwave spectroscopy. For some molecules, such as NH_3, this region probes the inversion modes. For H_2O and most other species, it is the pure rotational transitions that are investigated. As pressure broadening is a major contribution to an otherwise very narrow linewidth, microwave spectroscopy is regularly done in the gas phase at low pressure: typically 0.01 to 0.1 Torr. Therefore, a target molecule must have sufficient volatility or vapor pressure to reach these levels. In addition, the molecule must have a permanent dipole moment for rotational motion to affect or be affected by an electromagnetic field. Light molecules are preferred over

large ones to simplify the spectrum, unless the internal temperature of the molecule can be greatly cooled such as is possible in supersonic jet expansions. Large, heavy species have many low frequency vibrational modes appreciably populated at room temperature, leading to a very dense pure rotational spectrum with difficult line assignments near room temperature.[4]

The Water Molecule

Whether vapor or ice, at 30 or 3000 Kelvin, isotopically substituted or plain, ordinary $^1H_2^{16}O$, the water molecule is found throughout the universe.[5, 6, 7] Its presence is essential for a variety of chemical and physical reactions[8], from enabling life on Earth to enabling star formation. Despite the decades of work done on the molecule, our understanding of it is not complete, and any number of spectroscopic analyses continue. One good reason is the incredible density of lines. Water has ~85,000 vibrational transitions $\times$ a few hundred rotational levels per vibrational band $\times$ p, q, and r branches $\times$ combinations of ?k for each vib-rot transition $\rightarrow$ billions of lines.[10] The hope of this research was to add to the collected information by measuring some low-intensity transitions in the millimeter and submillimeter regions.

Water is an abundant interstellar species—probably the most abundant molecule in the universe after H2 and CO.[7] It is found in cool stars,[10-13] star-forming molecular clouds,[14] and cometary comae,[15] to name but a few environments. Its strong dipole moment and hydrogen-bonding capabilities enable it to exist as a liquid or solid over a range of physical conditions. Its known role in star forming regions is as a coolant when in the gas phase. The density and diversity of spectral lines in the infrared provide many channels for emitting photons after a collision, effectively converting thermal energy into

light.[16] Water is also the major constituent of the icy mantles coating interstellar grains in star-forming molecular clouds and the icy planetesimals[8] of the outer solar system. While the high temperature of medium stars like our Sun would preclude the stability of water molecules, in sunspots, oxygen-rich late type stars and brown dwarfs, at temperatures ~2000 K, water has been found. In some cases it is a very abundant constituent of (sub)stellar atmospheres.

Besides the straightforward H_2O molecule, deuterated water plays an important role in the cosmos as well. Despite its lower abundance (in the Orion cloud, for example, the HDO to H_2 ratio is ~ 10^{-7} – 10^{-9}, while $HDO:H_2O$ is ~0.004 – 0.01), [17] deuterium is ubiquitous and detectable.   It serves as a sensitive indicator of the origins and evolution of heavenly bodies. The HDO levels provide clues to whether comet formation took place primarily in a cold interstellar cloud, or a well-mixed solar nebula,[15] for example. Measurements of H_2O and HDO have also been used to infer the water content and temperature of the upper atmosphere of Venus,[18] and the fractionation and gas dynamics of the Martian atmosphere.[19] Coupled with atmospheric and solar models, the present day D/H ratios in planetary atmospheres can be used to estimate the original water inventory of terrestrial planets.

On the Differences between H_2O and HDO

While the substitution of one deuterium atom for one hydrogen atom in the water molecule introduces very small changes structurally, the mass increase has a large effect on the inertial, and therefore the rotational and vibrational, properties of the molecule. As shown in Table 1, the dipole moment is slightly different between the two molecules, whereas the moments of inertia are drastically different, as are the fundamental vibration

frequencies (transitions from the ground state to the first excited state of each mode illustrated in Figure 1.) In addition, the axes of the moments of inertia are skewed for HDO, having a profound effect on the allowed rotational transitions for the molecule. Since the dipole moment of H_2O lies along one of the inertial axes, it is only allowed those types of transitions, namely b-type. The dipole moment of HDO, on the other hand, has nonzero projections onto more than one axis, enabling it to have both a-type and b-type transitions, thereby increasing the potential range and number of spectral lines.

Table 1. Some properties of H_2O and HDO.[20]

	H_2O	HDO
Bond length x 10^8 (cm)	0.95718	0.9571
Bond angle	104.523°	104.529°
Dipole moment (Debye)	1.85498	1.85175
Moments of inertia x 10^{40} (g cm^2) *		
I_x	2.9376	4.2715
I_z	1.9187	3.0654
I_y	1.0220	1.2092
Transition bands from ground to vibrational state (cm^{-1})		
(100) or ν_1	3656	2726
(010) or ν_2	1594	1402
(001) or ν_3	3756	3703

The x axis passes through the molecular center of mass and is perpendicular to the plane of the molecule. In H2O, the z axis bisects the bond angle in the plane, and the y axis is perpendicular to the other two. In HDO, the z and y axes are rotated about the x axis by 21.09°.
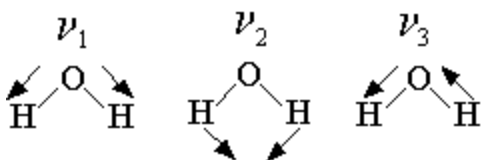

Figure 1. The vibrational modes of water: ν_1, symmetric stretch; ν_2, bend; ν_3, asymmetric stretch.

Spectral Data and Remote Sensing

Upon the advent of radioastronomy in the 1960s, humanity's knowledge of the universe changed drastically. For the first time the potential richness and diversity of chemistry in the interstellar medium was discovered. Before then observations of the night sky were limited to optical wavelengths—revealing stars, galaxies and some nebulae. Microwave remote sensing, however, revealed what the shorter wavelengths could not: molecules, some quite complex, in the material between stars. So far over 100 molecules, some composed of more than 10 atoms, have been identified, ranging from common small molecules like water (H_2O), ammonia (NH_3), and formaldehyde (H_2CO) discovered at the outset, to large organic species such as ethanol (C_2H_5OH) and $HC_{10}CN$, and prospective polyaromatic hydrocarbons.[21] While H is the most common atom in the universe, followed by He, C, O and N,[22] heavier elements formed by fusion in stars are detected as well in molecules: NaCl, AlF, SiS,[21] to give a few examples.

These discoveries sparked new theories about the nature of the composition of the universe. It is now believed that molecular clouds contain most of the mass of the ISM in gas rich galaxies such as our Milky Way. These clouds are large (1-100 light years across) and have temperatures of 10 – 600 K that depend sensitively on the rate at which young stars are being born within them. The average density is on the order of 10^2 - 10^3 cm^{-3}, but the clouds are inhomogeneous, with cores of dense material. These cores are often sites of active star formation, a process of great interest in astrophysics. Interstellar clouds contain material as gaseous molecules and as tiny dust particles, the latter comprising ~1% of the ISM mass with a size distribution peaking at ~0.1 μm.[22] These particles scatter and absorb the radiation from stars. This extinction has an inverse

wavelength dependence: optical wavelengths become scattered by dust, while longer ones get through relatively unchanged. Optical wavelength measurements detect little, while infrared, microwave and radio wave regions receive profound observations. In the coldest regions, only far-IR and microwave studies can be used, as summarized by Figure 2. The millimeter region of the spectrum is dominated by rotational transitions of polar molecules, some of which are strong enough to enable identification. Once identified and studied, astronomers are able to use molecular spectra to determine physical conditions (temperature, density, etc.) and probe inhomogeneities in these conditions. [For an excellent review paper on submillimeter astronomy please see reference 23.]
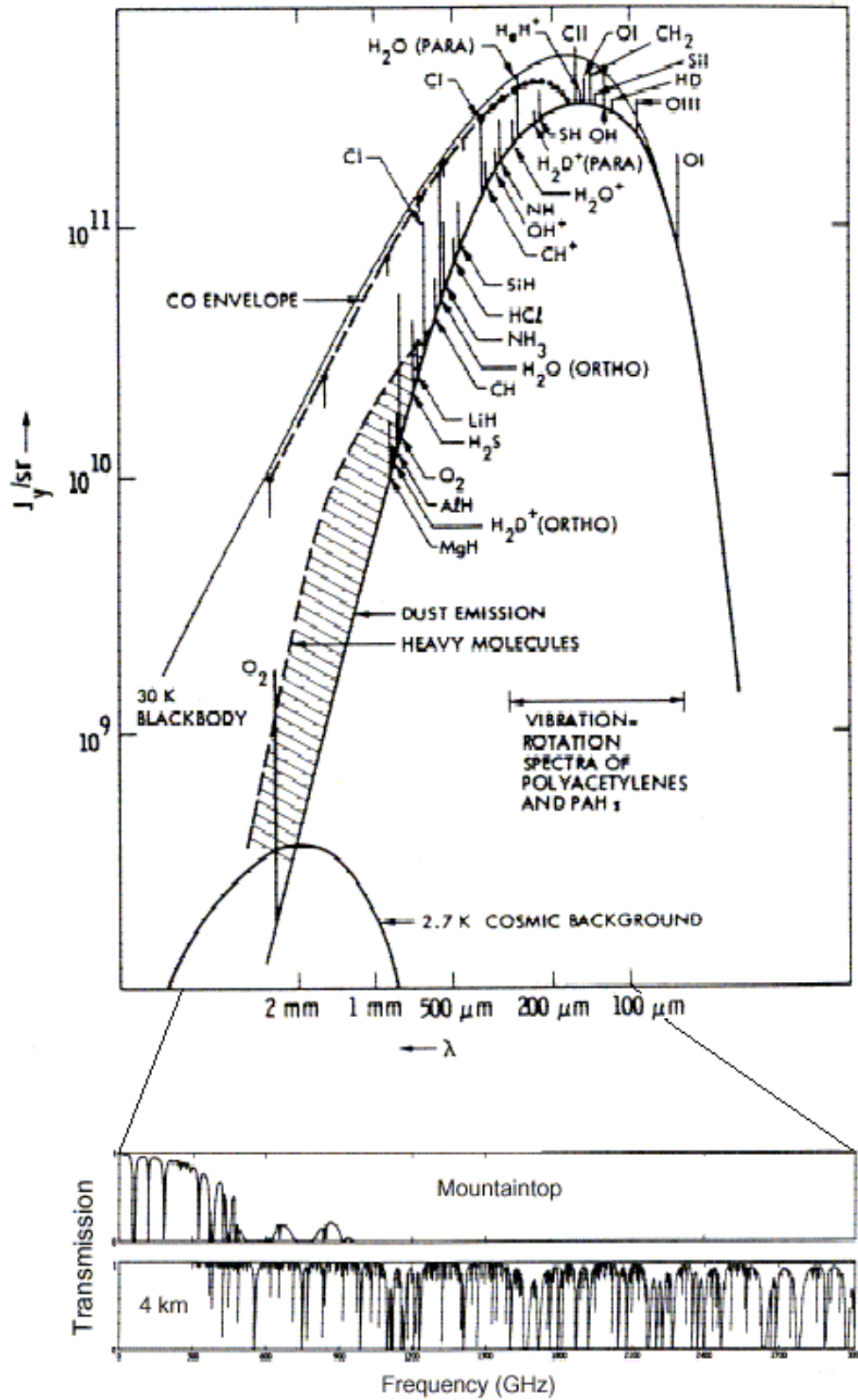
Figure 2. Molecular cloud spectrum, showing a continuum of dust particles, heavy molecules and individual small molecules.

The hardware, telescopes and detectors, for millimeter and submillimeter astronomical observations continue to improve in style and sensitivity. Due to the interfering effects of water in the earth's atmosphere, also outlined in Figure 1, ground-based observations in this band are often blocked. Windows from 0-300 GHz, around 650 GHz and 850 GHz, are accessible to high altitude telescopes, such as the 10.4 m Caltech Submillimeter Observatory on Mauna Kea, Hawaii. The upper atmosphere offers less interference. The Kuiper Airborne Observatory (which flew from the late 1970s to the early 1990s)[24] took advantage of the increased accessibility at an altitude of 12 km. The best observations are done outside of the Earth's atmosphere entirely with telescopes cooled to very low temperatures. The Infrared Space Observatory,[25] a mission of the European Space Agency that flew from Nov. 1995 to May 1998, using a 0.6 m telescope with a wavelength range of 2.5 to 240 μm, found water everywhere: the upper atmospheres of Jupiter, Saturn, and Uranus, the moon Titan, and in the Orion Nebula.

Two important upcoming missions will contain the latest in infrared observing technology. The SOFIA[26] (Stratospheric Observatory for Infrared Astronomy) mission, flying on a Boeing 747SP aircraft at 12 km altitude, will contain a 2.5 m telescope, and detection capabilities from 5 to 655 μm, is scheduled to begin flight operations in 2004 (Figure 3). Launching in 2007 is the Herschel space observatory[27] (formerly FIRST—the Far IR Space Telescope); outlined in Figure 4, its 3.5 m telescope directed to a high resolution spectrometer, camera and photometer, and will operate at a distance of 1.5 million kilometers from the Earth in the so-called L2 Lagrangian point.
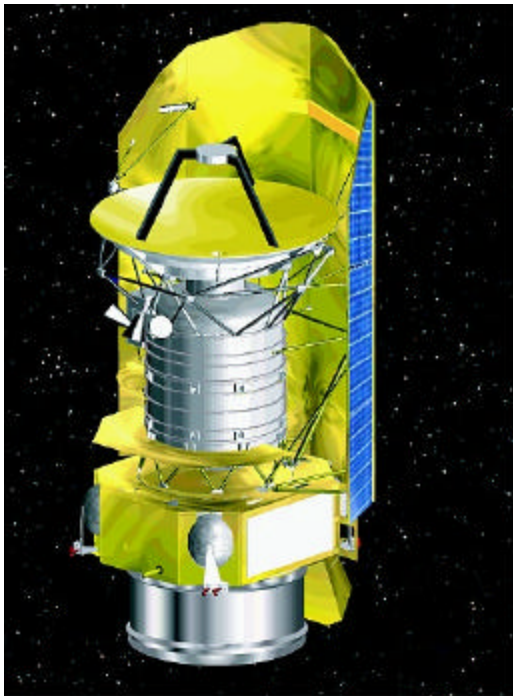
Figure 2. The SOFIA aircraft.

Figure 3. The Herschel Space Observatory.

As an individual astronomer fortunate enough to get time on these facilities can only observe for so many hours, prior knowledge of where to look for spectroscopic

features is essential. Predictive models have not yet reached an accuracy for use in microwave remote sensing; extensive laboratory measurements of center frequency and line-shape data is essential to the success of these missions, and motivates the research undertaken in this thesis.

On the Nature of Molecular Rotation

The rotational energy levels of a molecule are quantized. The simplest model to describe this behavior is that of a rigid rotor in free space, not influenced by any interactions with surrounding molecules. The rigid rotor model has been well studied, and simple molecules such as HF and CO show very structured, easily understood spectra. Water, on the other hand, is classified as an asymmetric top. Its three moments of inertia are all different, producing a spectrum that is dense, complex and apparently structureless. A brief introduction to the quantum mechanics of molecular rotation follows.

For a rigid rotor, the Hamiltonian for rotation is

$$\mathbf{H} = \mathbf{J}/2\mathrm{I}$$

where $\mathbf{J}$ is the angular momentum operator and I is the moment of inertia. In general, for a polyatomic molecule, $\mathrm{I} = \Sigma_i\, m_i R_i^2$ where m_i is the atomic mass and R_i is the distance of the ith atom from the molecular center of mass. The energy level solutions to the Hamiltonian depend on J:

$$E_J = (h2/2I)J(J + 1).$$

For a polyatomic molecule, consider the separate moments of inertia as the molecule rotates around the orthogonal x, y and z axes, and label these I_A, I_B, and I_C. (Most commonly, I_B is in the same direction as the dipole moment.) Spherical rotors

have $I_A = I_B = I_C$; examples include methane (CH_4) and sulfur hexafluoride (SF_6). If two of these moments of inertia are equal, the molecule is a symmetric rotor and can be either prolate ($I_A < I_B = I_C$, as in CH_3Cl) or oblate ($I_C > I_A = I_B$, as in benzene, C_6H_6). Most larger molecules, even those with a great deal of symmetry, are asymmetric rotors, with I_A ? I_B ? I_C. The Hamiltonian is then

$$\mathbf{H} = \mathbf{J}_A^2/2I_A + \mathbf{J}_B^2/2I_B + \mathbf{J}_C^2/2I_C.$$

The energy levels are further complicated, and split according to A, B and C. Changes in the internal angular momentum about the symmetry axis divide the main branches into the complex spectrum ordinarily seen. [For complete details and explanation of the asymmetric top Hamiltonian, please see references 28 and 29.]

The quantum number J and two pseudoquantum numbers K_a and K_c describe the rotational structure of an asymmetric rotor. For all molecules, J is the total angular momentum, with the selection rules ?J = 0, +1 or –1 producing the Q, R and P branches. For a symmetric top, the quantum number K is defined as the projection of J along the highest symmetry axis. Since no single angular momentum projection operator can describe the state of an asymmetric top with a given J value, K is split into the two pseudoquantum numbers K_a and K_c. K_a is the value of K in the limiting case of a prolate symmetric top, K_c for an oblate symmetric top. The selection rules are furthermore divided into two classes. For an A-type transition,

?K_a = 0, ±2, ±4, …

?K_c = ±1, ±3, …;

while a B-type transition has

?Ka = ±1, ±3, …

?Kc = ±1, ±3, ….[12]

HDO is a prolate symmetric rotor with both A-type and B-type transitions.[28]

The rigid rotor approximation is not perfect when one considers real molecules in space. An increased rotational energy is comparable to an increased rate of rotation, which changes the angular momentum. The centrifugal force is proportional to angular momentum squared, which causes the bonds to expand against the restoring force, distorting the molecule. The work done by centrifugal distortion must be subtracted from the rigid rotor energy. The energy levels are now, for a linear molecule

$$W(J) = BJ(J + 1) - DJ^2(J + 1)^2 + \ldots$$

and for a symmetric top

$$W(J, K) = BJ(J + 1) + (C - B)K^2 - D_J J^2(J + 1)^2 - D_{JK}J(J + 1)K^2 - D_K K^4.[1]$$

B, C are the rotational constants as before, and D, D_J, D_{JK}, D_K are centrifugal distortion constants, which depend on various molecular force constants and moments of inertia. Some of these force constants cannot always be determined from small amounts of experimental data, making their theoretical calculation difficult.

For linear molecules and symmetric tops, the change in line position from the ideal case is usually small, ~ 1 MHz or less.[4] Asymmetric rotors distort further, with errors reaching up to hundreds of MHz, especially for the high J levels accessible to some molecules. H_2O and HDO present extreme cases of centrifugal distortion thanks to the very large rotational constants involved, increasing the difficulty of spectral analysis[7, 30] and making even more important the careful experimental investigation of their rotational spectra. Fortunately, there is much useful information that can be gained from the

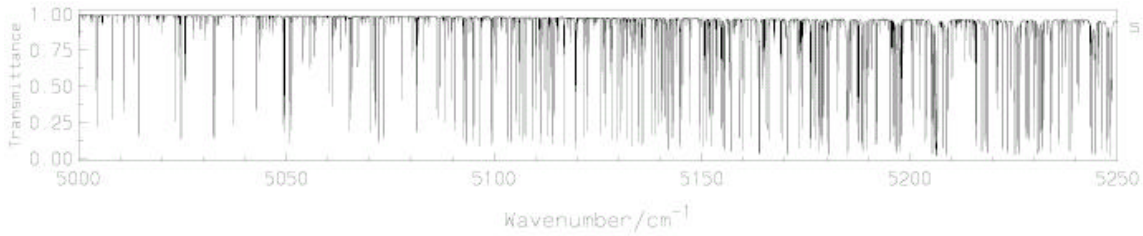spectrum of an asymmetric top without rigorous advanced mathematics or extensive labor.[31]

Figure 5. The infrared spectrum of H_2O in the range 5000-5250 cm^{-1}.[32]

Barely a fraction of the billions of potential spectroscopic transitions are detectable under laboratory conditions. This, still, is an extensive spectrum throughout the microwave and infrared regions, as can be seen in Figure 5. Conditions differ strongly in molecular clouds, including highly shocked regions of high temperature in the vicinity of star formation. As illustrated by Figure 6, theoretical predictions indicate a large increase of lines for water vapor. The a- and b-type transitions accessible for HDO will increase even more the spectral complexity at high temperatures.
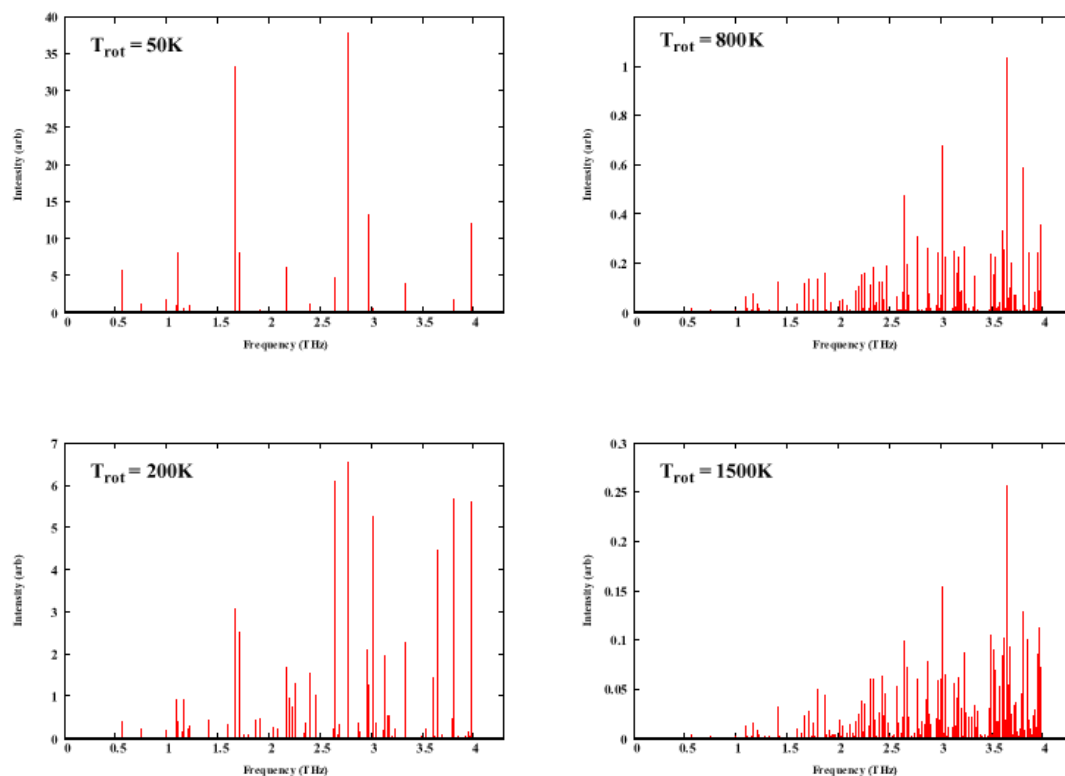
Figure 6. Predicted spectra of H2O vapor from 0.5 – 4 THz for rotational temperatures of 50, 200, 800 and 1500 K. While the intensity is arbitrary, the scaling factor is the same for all four plots, making the relative intensity meaningful.

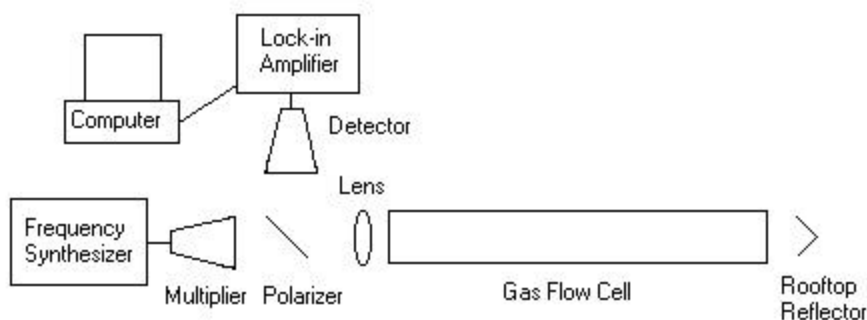*Details of the Hardware for Microwave Spectroscopy*

Figure 7. A flow cell setup for submillimeter spectroscopy.

Figure 7 illustrates the general setup of a millimeter or submillimeter spectrometer. Photons from a radiation source pass through a gas cell and enter a

detector. Sources are discussed below. The cell may be a variety of dimensions (the most common lengths seem to be 1-2 meters) and out of various materials. Molecules adhere differently to glass or metal, so the target molecule has some bearing on the type of cell used. The beam can be single pass, or, with the use of a rooftop reflector, double pass. Detectors are adapted from both the centimeter-wave region (crystals) or the infrared region (thermal).[4] Thermal detectors predominate submillimeter spectroscopy, such as the InSb hot electron bolometer at JPL. At liquid helium temperatures (4.2 K) absorption of radiation by free carrier electrons causes the mean temperature of the electrons to rise about that of the lattice. As electron mobility is proportional to temperature, an increase in temperature causes a change in conductivity. The low thermal mass of electrons combined with their short energy relaxation time leads to a fast and sensitive submillimeter detector.

In microwave spectroscopy, tunable sources with high stability, spectral purity and low phase noise are necessary for sensitive measurements. During the course of data collection, we attempted to use three different types of microwave sources: klystrons, backward-wave oscillator, and diode multipliers. Each type has its own particular characteristics in terms of design, power output, frequency range, and ease of use. What follows is a brief explanation of how each device works, and how well it works in the lab.

The klystron has been, until recently, the traditional source for microwave spectroscopy due to its low noise, high power, and nearly monochromatic output. It consists of two resonant cavities through which an electron beam passes. A radio frequency field in the first cavity bunches the electrons into groups. These pass through the second cavity, effectively inducing a second radio frequency field. The klystron

oscillates when some of this second RF energy is fed back to the first cavity. The output frequency is adjusted by mechanically changing the cavity size, usually simply by turning a screw. A reflector electrode can be substituted for the second cavity. Klystrons require a very stable high voltage power supply, and precise adjustment of several variables to obtain proper function. The frequency produced cannot be read directly; it must be compared to a known signal and the difference locked. The frequency range for each klystron is not very large—between 6 and 10 GHz—with variable power depending on the position within that range.[4]

The backward-wave oscillator, or BWO,[33] works on similar principles. An electron beam passes along a corrugated waveguide to a collecting anode, while an electromagnetic wave sent in at the anode moves toward the cathode. The wave interacts with the beam at regular intervals, bunching the electrons into groups, and moving the wave towards a higher frequency. By varying the electrode voltages one can control the frequency produced. Again, high voltages are required to control the electrons. The BWO at JPL has a large frequency range—from about 550 to 710 GHz—with adequate power to obtain sensitive measurements.

These two technologies have been replaced by a more compact and electrically efficient means of frequency generation. A multiplier takes as input a signal at a known frequency, and produces n harmonics of that frequency. A traditional synthesizer, enabling the end frequency to be calculated simply as $n \times$ the input frequency, usually produces the input. Without going into semiconductor physics, a diode mixer or multiplier is a circuit that takes two signal inputs and forms an output at the sum and difference frequencies according to the trigonometric relation

$$\cos \omega_1 t \cos \omega_2 t = \tfrac{1}{2} \cos (\omega_1 + \omega_2)t + \tfrac{1}{2} \cos (\omega_1 - \omega_2)t.$$

Given two signals at f_1 and f_2, one receives two output signals at $f_1 + f_2$ and $f_1 - f_2$. Knowing this, if the two signals have the same frequency, the circuit is effectively a doubler. One can also see how all manner of other harmonics can be formed. One of the common ways of making this type of mixer is using simple nonlinear transistor or diode circuits,[34] often Schottky,[35] Gunn or whisker contacted diodes. Resistive diode frequency multipliers are less efficient than varactor multipliers, but are much more broadband, easier to tune, and have better coupling between the input radiation and the diodes.[36] Much development is being put into mixers with very good noise sensitivity and little power conversion loss. Multipliers of this sort offer a source with a large frequency range ($\sim 50 - 100$ GHz), easily tunable power over that range, relatively low noise, and a compact structure allowing it to be placed easily within the experimental setup. Compared to direct oscillators, multipliers put out less power, but when combined with sensitive, cryogenic detectors are capable of high sensitivity millimeter and submillimeter measurements.

The measurements presented here were made in the millimeter and submillimeter spectroscopy facility at the NASA Jet Propulsion Lab. Two separate multiplier chains (x24, x30, x36 or x42) were used to obtain the frequencies between 200 and 750 GHz. The chains consisted of a Hewlett Packard sweep synthesizer followed by an active HP sextupler. The second multiplier in the series was either a Custom Microwave whisker-contacted diode multiplier or an anti-parallel planar Schottky diode multiplier built at JPL, the latter biased to 200 mV if even harmonics were desired. The beam passed twice through a 1 m long, 7.3 cm diameter glass absorption cell, pictured in figure 8, before being reflected into a liquid helium cooled InSb hot electron bolometer detector. [Please see references 37-39 for further information on this spectrometer and its capabilities.] A mixture of 10:1 D_2O:H_2O (so that protons would be the limiting reagent) was connected to the flow cell, which was kept at a pressure of 10-30 mTorr. Experiments measuring the spectrum of perchloric acid were done concurrently, and while the cell was pumped down to minimum pressure before beginning an HDO run, water, with its high polarity, tends to remove molecules adsorbed to the glass walls. However, HDO was allowed to flow for several minutes before any measurements were taken, and contamination error was not a factor in the characterization of any measured lines of HDO reported here.
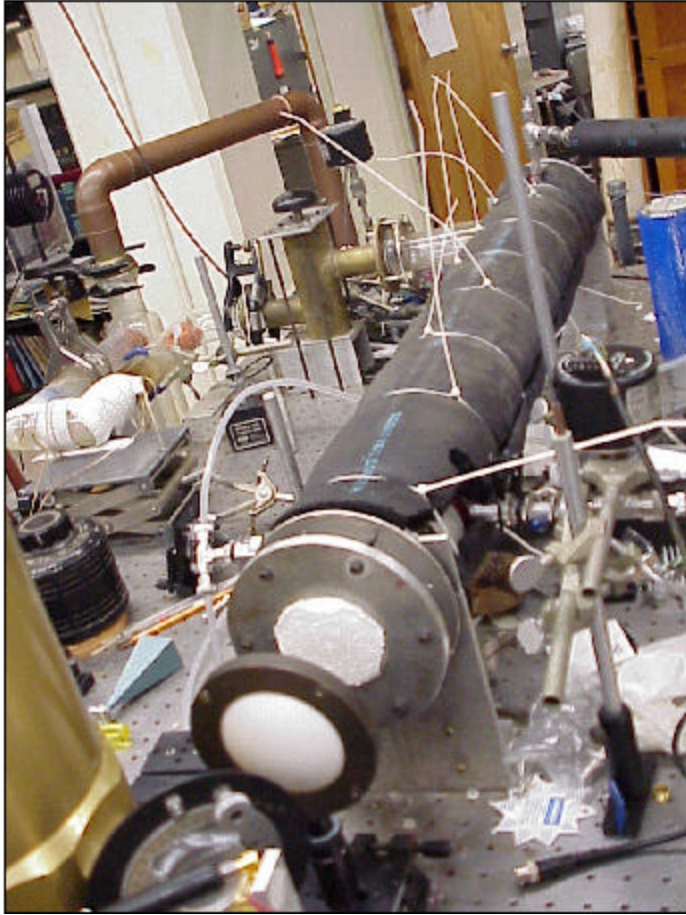
Figure 8. The flow cell at JPL.

Results

The following table lists the frequencies of 9 previously unreported lines measured with the JPL microwave spectrometer. Linewidths were ~ 1 MHz. Parameters of the peak fitting program make exact peak assignment somewhat arbitrary, but these values should be accurate to 100 kHz or less. For comparison, the line frequencies predicted from two previous HDO analyses are included. As can be seen, the differences between the predicted and measured values greatly exceed the experimental error bars.

Table 2. Measured transitions of HDO

Lower	Upper	Observed	Pearson[a, 40]	Toth[b, 41]
14 5 9 0	14 5 10 0	210133.925	210120.393	210129.031
7 2 5 0	8 0 8 0	228072.391	228073.364	228073.108
8 4 4 0	9 2 4 0	232312.291	232311.578	232314.572
13 3 10 0	14 2 13 0	429811.772	429812.689	429813.346
12 2 11 0	11 3 8 0	443173.868	443174.779	443172.098
12 4 8 0	12 4 9 0	468101.974	468105.88	468100.741
9 1 8 0	8 3 5 0	717695.816	717698.123	717695.05
2 0 2 1	1 1 1 1	434517.764	434517.754	434520.987
2 1 1 1	2 0 2 1	671641.716	671641.712	671640.033

a: predictions made by Pearson using the line-fitting programs SPFIT and SPCAT
b: predictions made by calculating the energy differences between the rotational energy levels as measured by Toth.

In addition to these lines, a number of interesting doublet transitions whose predicted intensities were within sensitivity limits were searched for, but not found.

Table 3. Doublet transitions of HDO

Lower	Upper	Pearson[a, 40]	Toth[b, 41]
16 8 9 0	15 9 6 0	324179.164	324221.346
16 8 8 0	15 9 6 0	324491.158	324520.539
12 8 5 0	13 7 6 0	365046.949	365039.588
12 8 4 0	13 7 7 0	365382.771	365379.553
13 8 6 1	14 7 7 1	437777.829	437783.928
13 8 5 1	14 7 8 1	438566.389	438571.483
15 10 6 0	16 9 7 0	446410.105	
15 10 5 0	16 9 8 0	446421.272	
13 6 8 0	12 7 5 0	472143.709	472144.341
13 6 7 0	12 7 6 0	479985.132	479984.214
15 7 9 0	14 8 6 0	635220.981	635229.339
15 7 8 0	14 8 7 0	637796.21	637800.360

There are a few reasons why the lines could not be observed with the current setup. First, the actual intensity could be much smaller than predicted, beyond our limits of sensitivity. More power and a higher signal to noise ratio in these regions would be necessary. Also, the measurements were done at room temperature. With a higher temperature, possibly using an electric discharge cell of the type that is used to produce far-IR water lasers, there will be a larger population in the higher J states. Finally, the line prediction could be incorrect. These transitions have high values of J and K, were the fits tend to break down due to numerical and physical effects. Due to the weakness of the lines, only small regions around the predicted frequency could be examined with high sensitivity.

A full catalogue of spectral lines for HDO and other molecules is available online at http://spec.jpl.nasa.gov.

On Modeling and Fits

As the instrumentation for spectroscopy developed, spectra could be measured to ever higher degrees of accuracy without needing to know what, exactly, was being observed.[44] In the laboratory, where the molecule was known or at least suspected (in the case of transient species), the transitions corresponding to each spectral line were in question. In remote sensing, it is often the molecule itself that has not been identified. More broadly, to have a complete understanding of the physical nature of a molecule, and its behavior in various environments, it is important to have as much information as possible. To solve these problems, it is desirable to construct quantitative models with which to calculate molecular spectra under a variety of conditions.

The advantages of a model are numerous. If the calculations can be made sufficiently accurate, one could make useful predictions for as yet unobserved transitions. In the case of water, as an asymmetric rotor with a number of levels due to K splitting, there are an enormous number of lines throughout the GHz and THz regions. Accurate predictions of these lines make laboratory and astronomical observations much more efficient and successful.

The construction and calculation of energy levels by hand for the simplest molecules, such as H_2, can be accomplished, though the calculations are incredibly time-consuming and tedious. For anything more complex, calculations by hand are impossible, and still difficult even when using a computer. A number of scientists have created predictive models and fits using a wide variety of techniques to apply to the water molecule and its various isotopomers. Despite the abundance of measured spectra, *ab initio* calculations, experimental and theoretical potential energy surface calculations,[45]

and so forth, the ability to accurately predict transitions for astronomical heterodyne observations has not yet been reached. However, development continues, and combinations of theory and experiment allow us to obtain the maximum of information from observed spectra.

In spite of its simple structure, water is an especially complicated molecule to model. Pure rotational motion in an idealized sense is almost absent—rotational energies meet that of the lowest vibrational energy level at $J = 8$. This introduces an extremely strong centrifugal distortion due to bending-rotational coupling, especially for the $\nu 2$ states.[46] Anharmonic and Coriolis resonance interactions between the vibrational states add further perturbations to a rigid rotor spectrum.

Traditionally, rotational states of water are fit spectroscopically using a standard Hamiltonian, including centrifugal distortion terms,[9] then expanded with a power series, of the example form:

$$F(x) = x^p?\, a_k x^k$$

The summation runs from $k = 0$ to 8, and a is a scalar with alternating signs. Such perturbation approaches work for most molecules with only a few terms needed in the centrifugal distortion series. For water (and HDO), however, a rotational power series tends not to converge beyond $K = 10$ and $J = 20$, and so for accurate predictions of the higher energy states such as will be populated in warm regions of molecular clouds or planetary atmospheres, a different approach is necessary.

The Euler series is similar in approach to a power series, but with a useful difference.

$$z = x/(1+x) \qquad f(x) = x^p/(1+x)\ ?\, b_k z^k$$

Again, the summation runs from k = 0 to 8, and b is a scalar. Rather than drive convergence using alternating signs to the summation, there is a limiting factor in the denominator. In calculations of ln x, for example, this method provides results much closer to the true value than a power series expansion for a limited number of terms.

The fit program used here consists of two major programs written in FORTRAN, and developed by Dr. H.M. Pickett and his group at JPL. The first, SPFIT, compares assigned transitions to the parameters of a model Hamiltonian,[46] using non-linear regression to minimize the root mean square (rms) error. The Euler series outlined above is applied in Hamiltonian calculations for the molecule, leading to a series of output parameters, $D_{k,n}$ and $d_{k,n}$:

$$D_{k,n} = (\mathbf{P}_a^{2k}[\mathbf{P}^2 - \mathbf{P}_a^2]^n)/([1 + (a\text{-}b)\mathbf{P}_a^2 + b\mathbf{P}^2]^{k+n})$$

$$d_{k,n} = \{(\mathbf{P_a}^{2k}[\mathbf{P}^2 - \mathbf{P_a}^2]^n)/([1 + (a\text{-}b)\mathbf{P}_a^2 + b\mathbf{P}^2]^{k+n+1}), \mathbf{P}_b^2 \text{-} \mathbf{P}_c^2\}.^{[47]}$$

where $a - b = 2H_K/D_K$, $b \sim 2H_J/D_J$; P is the angular momentum operator; $\mathbf{P}_a$, $\mathbf{P}_b$, and $\mathbf{P}_c$ are projections of $\mathbf{P}$ onto the molecular coordinate system, and { } is the anti-commutator. The parameters $a - b$, b are created using a power series at low J, K. $D_{k,n}$ and $d_{k,n}$, which have little physical meaning, are implemented into the second program, SPCAT, that is used to predict frequencies and intensities at room temperature. Partition functions are also generated for a wide range of other temperatures to enable extensive simulations of molecular rotational spectra.

Of the lines measured in this work (see Table 2), several have substantial root mean square (rms) deviations from the predictions of Pearson and Toth. While a difference of, for example, 4.9 MHz is small compared to the total line frequency of 200-700 GHz, it is roughly 50 times the estimated experimental error. In addition, a small

difference in line frequency can have a large impact on astronomical remote sensing experiments. The differences in the residual patterns of the previous fitting efforts are important.

Toth based his work (see references 41-43) on infrared and far-infrared Fourier transform spectroscopy (FTS), which access a very large number of lines, but at a low spectral resolution (~30 – 100 MHz), with line centers being measured to approximately one tenth of this resolution. Therefore the errors are relatively random: essentially independent of the J, K values obtained in this work. FTS alone has insufficient precision to be used as a basis for astronomical spectroscopy. For observations of molecular clouds, the line density is such that line position must be known to 1 MHz at 300 GHz (or a fraction of a km/s in velocity space.)

Pearson's work combined the FTS measurements of higher J, K states with high resolution (sub)millimeter measurements of the type outlined in this work. The fitting program allows the data sets to be weighted by their relative precisions. Thus fits can utilize the best of both approaches: high precision measurements for a few lines via submillimeter spectroscopy, and wide spectral energy coverage with FTS. The errors of the Pearson fit are thereby more structured than those of Toth. RMS values are near the submillimeter experimental uncertainty for low J, K lines, and grow by factors of nearly ten for lines constrained only by FTS measurements.

As we have expanded the range of J, K values obtained with a high precision technique, the fit must correspondingly be redone. In a preliminary work augmenting the approach of Pearson, we have been able to drop the rms for the nine lines studied here from 4.9 to 0.5 MHz. Low J, K lines are predicted to within experimental uncertainty,

and the rms for the higher excitation lines has been improved greatly. While residual error is still 2-3 times larger than the estimated experimental uncertainties, we hope further efforts with the fits will improve this. Nonetheless, with the addition of these lines to the high precision spectral database, the lines of HDO accessible by astronomers can be predicted to adequate precision to enable reliable assignments in all but the hottest environments.

Conclusions and Future Directions

We have successfully measured nine uncatalogued lines, seven in the vibrational ground state (000) and two in the first excited bending state (010) of HDO. A least-squares regression analysis of these lines, added to the existing data, resulted in molecular parameters whose values are in excellent agreement with the best previously existing analyses but which do a much better job of reproducing the higher J, K lines measured here. These lines will, hopefully, be added to the existing spectral catalogue of HDO, so that they may be of benefit to further spectroscopic analysis.

Several other lines of interest were sought for, but not found. If it is the case that their intensity is much lower than predicted, then improved sensitivity is needed. The next generation of diode multipliers may provide enough power at these frequencies to improve the signal-to-noise, revealing new transitions. An alternate method would be to increase the sample temperature drastically, populating the high J states, so that their spectrum may be more easily observed. In addition, the development of instrumentation to probe the THz region of the spectrum is ongoing, and will further our understanding of the HDO molecule.

While the lines were added to the program SPFIT, which generates parameters for use in spectral line prediction, these parameters have not yet been used to augment the existing data for use in SPCAT predictions. Some time could also be spent further adjusting the parameters of the fit, to ensure the lowest least-squares error possible.

References

1. King, <u>Spectroscopy and Molecular Structure</u>, Holt, Rinehart & Winston, Inc., 1964.

2. Levine, <u>Molecular Spectroscopy</u>, John Wiley & Sons, 1975.

3. Shostak, Ebenstein, Muenter, "The dipole moment of water," J. Chem. Phys 94 (9) 5875-5881 1991.

4. Townes & Schawlow, <u>Microwave Spectroscopy,</u> Dover Publications, Inc., 1975.

5. Polyansky *et al*, "K-Band spectrum of water in sunspots," Astrophys. J 489 L205-L208 1997.

6. Pearson *et al*, "Millimeter- and submillimeter-wave spectrum of highly excited states of water," Astrophys. J 379 L41-L43 1991.

7. Bernath, "The spectroscopy of water vapour: Experiment, theory and applications," Phys. Chem. Chem. Phys. 4 1501-1509 2002.

8. Chen *et al*, "Submillimeter-wave measurements and analysis of the ground and ν_2 = 1 states of water," Astrophys. J. Supp. 128 371-385 2000.

9. Jørgensen *et al*, "H_2O in stellar atmospheres," Astron. & Astrophys. 372 249-259 2001

10. Polyansky *et al*, "High temperature rotational transitions of water in sunspot and laboratory spectra," J. Mol. Spec 186 422-477 1997.

11. Oppenheimer *et al*, "Infrared spectrum of the cool brown dwarf GI 229B," Science 270 1478-1479 1995.

12. Jones *et al*, "Water vapour in cool dwarf stars," Mon. Not. R. Astron. Soc. 277 767-776 1995.

13. Hinkle & Barnes, "Infrared spectroscopy of Mira variables. II. R Leonis, the H_2O vibration-rotation bands," Astrophys. J. 227 923-934 1979.

14. Moneti, Cernicharo, Pardo, "Cold H_2O and CO ice and gas toward the galactic center," Astrophys. J. 549 L203-L207 2001.

15. Bockalee-Morvan *et al*, "Deuterated water in comet C/1996 B2 (Hyakutake) and its implications for the origin of comets," Icarus 133 147-162 1998.

16. Nisini, "Water's role in making stars" Science 290 (5496) 1513-1514 2000.

17. Pardo *et al*, "Deuterium enhancement in water toward Orion IRc2 deduced from HDO lines above 800 GHz," Astrophys. J. 562 799-803 2001.

18. Encrenaz *et al*, "The thermal profile and water abundance in the Venus mesosphere from H_2O and HDO millimeter observations," Icarus 117 162-172 1995.

19. Bertaux & Montmessin, "Isotope fractionation through water vapor condensation: the Deuteropause, a cold trap for deuterium in the atmosphere of Mars," J Geophys Res-Planet 106 (E12) 32879-32884 2001.

20. Eisenberg & Kauzmann, The Structure and Properties of Water, Oxford University Press, 1969.

21. Winnewiser, "Interstellar and laboratory spectroscopy in the terahertz region," J. Mol. Struct. 408/409 1-10 1997.

22. Herbst, "Chemistry in the interstellar medium," Annu. Rev. Phys. Chem 46 27-53 1995.

23. Phillips & Keene, "Submillimeter Astronomy," Proc. IEEE. 80 (11) 1662-1677 1992.

24. http://spacelink.nasa.gov/NASA.Projects/Space.Science/Solar.System/Kuiper.

    Airborne.Observatory

25. http://www.iso.vilspa.esa.es/

26. http://sofia.arc.nasa.gov/

27. http://astro.estec.esa.nl/SA-general/Projects/First/first.html

28. De Lucia *et al*, "Millimeter and submillimeter wave rotational spectrum and centrifugal distortion effects of HDO," J. Chem. Phys. 55 (11) 5334-5339 1971.

29. Coudert, "Analysis of line positions and line intensities in the ν_2 band of the water molecule," J. Mol. Spec. 181 246-273 1997.

30. Baskakov *et al*, "New submillimeter rotation lines of water," Opt. Spectrosc. 63 (5) 600-601 1988.

31. Gordy & Cook, Microwave Molecular Spectra, John Wiley & Sons, 1984.

32. Mikhailenko *et al*, "Water spectra in the region 4200-6250 cm^{-1}," J. Mol. Spec. 213 91-121 2002.

33. Krupnov, "Phase lock-in of mm/submm backward wave oscillators: development, evolution, and applications," Int. J. Infra. Milli. Waves 22 (1) 1-17 2001.

34. Horowitz & Hill, The Art of Electronics, Cambridge University Press, 1999.

35. Oswald *et al*, "Planar diode solid-state receiver for 557 GHz with state-of-the-art performance," IEEE Micro. Guided Wave Lett. 8 (6) 232-234 1998.

36. Schitov *et al*, "Frequency multipliers for extension of frequency range of millimeter wave synthesizers," Int. J. Infra. Milli. Waves 21 (9) 1479-1488 2000.

37. Drouin *et al*, "Further investigations of the ClO rotational spectrum," J. Mol. Spec. 207 4-9 2001.

38. Müller, Miller, Cohen, "Rotational spectrum and molecular properties of bromine dioxide, ObrO," J. Chem. Phys. 107 (20) 8292-8302 1997.

39. Birk *et al*, "Rotational spectrum and structure of chlorine peroxide," J. Chem. Phys. 91 (11) 6588-6597 1989.

40. John Pearson, personal communication.

41. Toth, "HDO and D_2O low pressure, long path spectra in the 600-3100 cm^{-1} region," J. Mol. Spec. 195 73-97 1999.

42. Toth, "Air- and N2-broadening parameters of HDO and D_2O, 709-1936 cm^{-1}," J. Mol. Spec 198 358-370 1999.

43. Toth, "$HD^{16}O$, $HD^{18}O$ and $HD^{17}O$ transition frequencies and strengths in the ν_2 bands," J. Mol. Spec. 162 20-40 1993.

44. Tennyson, "Why calculate the spectra of small molecules?" Chem. Soc. Faraday Trans. 88 (22) 3271-3279 1992.

45. Polyansky, Jensen, Tennyson, "Potential energy surface of $H_2^{16}O$," J. Chem. Phys. 105 (15) 6490-6497 1996.

46. Pickett "The fitting and prediction of vibration-rotation spectra with spin interactions," J. Mol. Spec. 148 371-377 1991.

47. Pin Chen, Herb Pickett, personal communication.